Deep-Sea Research II 58 (2011) 1436–1450

Contents lists available at ScienceDirect

Deep-Sea Research II

journal homepage: www.elsevier.com/locate/dsr2

Phytoplankton composition and abundance in relation to free-floating Antarctic icebergs

Adrián O. Cefarelli [a,*], María Vernet [b], Martha E. Ferrario [a,c]

[a] Departamento Científico Ficología, Facultad de Ciencias Naturales y Museo, Universidad Nacional de La Plata, Paseo del Bosque s/n, 1900 La Plata, Argentina
[b] Integrative Oceanography Division, Scripps Institution of Oceanography, University of California San Diego, La Jolla CA 92093-0218, USA
[c] CONICET, Consejo Nacional de Investigaciones Científicas y Técnicas, Av. Rivadavia 1917, (1033) Buenos Aires, Argentina

ARTICLE INFO

Available online 21 December 2010

Keywords:
Antarctica
Iceberg
Meltwater
Phytoplankton
Diatoms

ABSTRACT

Free-drifting icebergs in the Weddell Sea are expected to affect the surrounding marine ecosystem. Sampling associated with iceberg C-18a, a large tabular, free-drifting iceberg in the NW Weddell Sea, carried out from 10 March to 7 April 2009, was designed to test the hypothesis that the iceberg's presence modified phytoplankton composition and abundance. Areas that define a gradient of possible iceberg influence were sampled for phytoplankton: stations close (<1 km) and far (18 km) from iceberg C-18a, an area with numerous small icebergs, Iceberg Alley, and a control site 74 km away. Quantitative samples were obtained from Niskin bottles and counted with an inverted microscope for species abundance. Qualitative samples were collected with nets from the ship's seawater intake. Taxonomic determinations were performed with light and electron microscopy. Overall, diatoms dominated in the mixed layer (surface-$\sim$40 m) and unidentified small flagellated and coccid cells at depth ($\sim$100 m). *Fragilariopsis nana*, a diatom 2.4–15.5 μm in length, dominated numerically the phytoplankton and was most abundant at the control area. The iceberg's effect on phytoplankton composition was consistent with the hypothesis that they facilitate phytoplankton communities enriched in diatoms, as found in other productive areas of Antarctica. Near the iceberg, diatoms were most abundant, principally at depth, while small flagellate concentration diminished. However, total phytoplankton abundance was lowest at Iceberg Alley in the area of highest meltwater contribution, as indicated by low mean temperature in the mixed layer, and highest at the control site. These results suggest that during austral fall, low growth or high zooplankton grazing could be counteracting the positive effect by icebergs on phytoplankton biomass, otherwise observed in summer months.

1. Introduction

Most phytoplanktonic studies on the influence of ice in Antarctic waters are related to the ice edge zones, the seasonal sea ice and the processes of melting (Smith and Nelson, 1985; Fryxell and Kendrick, 1988; Vernet et al., 2008). Taking into account the frequent iceberg calving from Antarctica ice shelves and the evidence that these events are increasing, there is little knowledge about their possible ecological impacts (Jacobs et al., 1979; Arrigo et al., 2002; Long et al., 2002). Studies on Antarctic icebergs (Ballantyne, 2002; Schodlok et al., 2006) present mostly physico-chemical processes, many of them modelling the structure of icebergs and describing their trajectory through time and space. The suggestion that icebergs could contribute with dissolved iron was first observed in the Antarctic Polar Front (de Baar, 1995). Icebergs can also affect the biological characteristics of the surrounding pelagic ecosystems with negative (Arrigo et al., 2002) as well as positive consequences (Smith et al., 2007). It has been suggested that the icebergs' effect could depend on the initial oceanic and ecological characteristics of the areas they travel (Schwarz and Schodlok, 2009). An iceberg traversing the nutricline and pycnocline could mix and introduce micronutrients to surface waters; in addition, freshwater produced by melting icebergs would generate an upwelling effect in the adjacent waters (Neshyba, 1977). The iceberg's net effect will be function of the balance between phytoplankton growth and dominant physical and biological forcing.

The presence of an iceberg of about 10,000 km^2 in southwestern Ross Sea showed, through satellite images, a noticeable diminution in chlorophyll *a* concentration and primary production during spring and summer by restriction of the normal drift of the pack ice and the consequent reduction of light availability (Arrigo et al., 2002). On the other hand, during late spring in the northwest Weddell Sea, Smith et al. (2007) found an increase of chlorophyll *a* concentration in the immediate vicinity of two free-drifting

* Corresponding author. Tel.: +54 221 4257744; fax: +54 221 4257527.
E-mail address: acefarelli@fcnym.unlp.edu.ar (A.O. Cefarelli).

0967-0645/$ - see front matter © 2010 Elsevier Ltd. All rights reserved.
doi:10.1016/j.dsr2.2010.11.023

icebergs. They reported that the microphytoplankton, characterized principally by the presence the diatoms, was the highest contributor to total chlorophyll *a* within 1.0 km distance around the icebergs and suggested that physical and chemical processes, such as mixing or the release of micronutrients, might be stimulating primary production. Similarly, Schwarz and Schodlok (2009) reported that waters affected by the passage of icebergs could increase phytoplankton biomass, measured as chlorophyll *a*, by as much as a third, and the effect was observed at the height of the austral growth season, from November to January.

High rates of primary production in the Weddell Sea are found in coastal waters and the ice edge (Garrison et al., 1987; Hegseth and von Quillfeldt, 2002; Kang and Fryxell, 1993). Large phytoplankton, mostly dominated by diatom species or microplankton (>20 μm), are commonly associated with these productive areas (Fryxell, 1989; Kang and Fryxell, 1993). The nanoplanktonic diatoms (2–20 μm) such as *Fragilariopsis cylindrus* also make important contributions to biomass and primary production in the Southern Ocean (Kang and Fryxell, 1991). *Fragilariopsis* is one of the best represented diatom genus in Antarctica and *Fragilariopsis* species can dominate phytoplankton and particularly diatom assemblages (Garrison et al., 1987; Estrada and Delgado, 1990; Hasle and Medlin, 1990; Round et al., 1990; Kang and Fryxell, 1992, 1993; Villafañe et al., 1995; Socal et al., 1997; Hegseth and von Quillfeldt, 2002). Small unidentified phytoflagellates, cryptophytes, prasinophytes and the prymnesiophyte *Phaeocystis* spp. are also important constituents of Antarctic phytoplankton usually present everywhere (Kopczynska, 1988, 1992; Garibotti et al., 2003).

Although several studies have approached the possible biological influence of icebergs in Antarctic waters (e.g., Smith et al., 2007; Schwarz and Schodlok 2009), none of them has attempted to characterize taxonomically and quantitatively the phytoplankton composition in relation to free-floating icebergs. The objective of this study is to identify, describe and quantify, by means of light and electron microscopy, the phytoplanktonic organisms found in the water column around an iceberg in comparison with unaffected waters. The sampling was carried out in the Powell Basin, northwestern Weddell Sea. We evaluate quantitatively the possible differences between four different areas with differing iceberg influence.

2. Materials and methods

Phytoplankton analysis is based on qualitative and quantitative samples obtained in four areas of the Powell Basin, northwestern Weddell Sea (Fig. 1) during the Iceberg III cruise (Smith, 2011). Between 10 March 2009 and 1 April 2009 we sampled around iceberg C-18a in its north east trajectory along the western edge of the Weddell Gyre at an average speed of 2 knots (Helly et al., 2011). Samples are grouped as near iceberg C-18a (0.3–1 km) and far (16–18 km) from the iceberg. A control site 74 km East of C-18a was visited twice, between 3 and 7 April 2009. A fourth area with numerous small icebergs, Iceberg Alley, located at the southern corner of the Powell Basin (>74 km from C-18a position), was sampled between 4 and 5 April 2009 (Table 1). Phytoplankton was collected with a 20 μm mesh net from the ship's seawater intake (9 m depth). Water was obtained with a Conductivity-Temperature-Depth (SeaBird SBE-45 CTD) sensor with a rosette outfitted with 24 8.5-L Niskin bottles, a Wetlabs ECO fluorometer and a C-Star transmissometer from Wetlabs. Samples were taken from the surface (0–2.5 m), ~25 m (25 ± 5.02 m) within the mixed layer, ~40 m (40 ± 5.6 m) at the base of the mixed layer, and ~100 m (102 ± 8.7 m) at the depth of the temperature minimum or winter water (Stephenson et al., 2011).

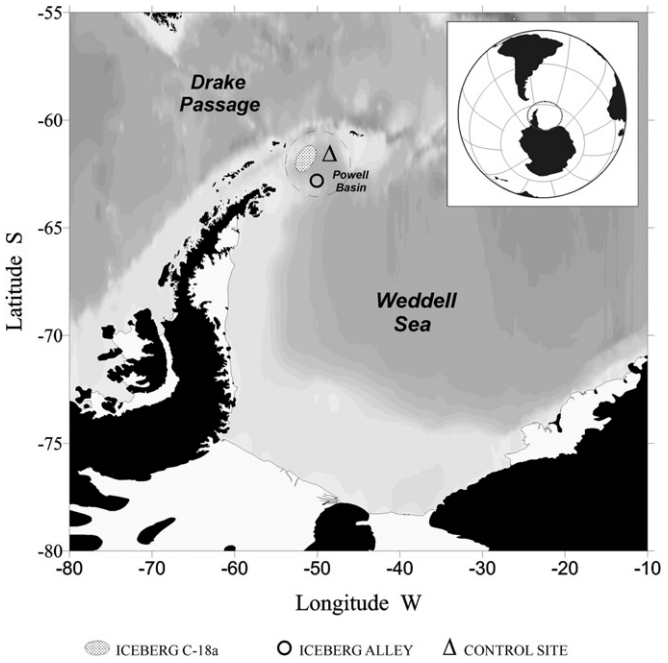

Fig. 1. Map showing the sampling areas in the Powell Basin, northwestern Weddell Sea. Effects of icebergs on phytoplankton were studied in Iceberg Alley (southwest Powell Basin) and C-18a (western Powell Basin). The iceberg C-18a area included two subareas: near C-18a and far C-18a (0.3–1.0 km and 16–18 km away from C-18a iceberg, respectively). Control site is at the mouth of the basin. (Map courtesy of Hernan Isbert Perlender)

All samples were preserved with Lugol's iodine solution. A first floristic analysis of fresh samples was done during the cruise with a Nikon E800 light microscope (LM) equipped with a digital camera, providing preliminary identification of the different taxa on water mounts. To identify individual cells at the lowest possible taxonomical level, diatoms and silicoflagellates not cleaned and cleaned of organic matter (Hasle and Fryxell, 1970) and mounted on permanent glass slides using Naphrax medium (Ferrario et al., 1995) was examined at the university's lab with a phase contrast Leica DM 2500 light microscope (LM) equipped with a Leica DFC420 digital camera. For more in-depth studies of diatoms, the material, mounted on stubs and coated with gold-palladium according to Ferrario et al. (1995), was examined with a Jeol JSM-6360 LV scanning electron microscope (SEM). Permanent slides were deposited at the LPC Herbarium of the Departamento Científico Ficología, Facultad de Ciencias Naturales y Museo, Universidad Nacional de La Plata, La Plata, Argentina.

To estimate cell abundance, quantitative samples were examined at 400X magnification with an Iroscope SI-PH inverted microscope (Utermöhl, 1958). Previously, 100 ml of each sample had settled for 48 h in sedimentation chambers. At least 300 individuals were counted in random fields, and the results expressed as numbers of cells per litre of water. Except for the empty frustules of the diatom *Leptocylindrus mediterraneus*, only live cells containing full chloroplasts were included in this study.

The biomass of the numerically dominant taxon (the diatom *Fragilariopsis nana*) was calculated according to the formula proposed by Montagnes et al. (1994), with the purpose of assessing its contribution to total phytoplankton biomass, measured as chlorophyll *a* (chl *a*). Forty two specimens of *F. nana* were measured with SEM, a mean size value was estimated for the species and used for the cell volume calculation. The geometric shape adopted was that of a rectangular box (Hillebrand et al., 1999).

The concentrations of chl *a* and phaeopigments was estimated fluorometrically (Holm-Hansen et al., 1965). Water aliquots were

Table 1
Stations and physical properties studied in NW Weddell Sea in March and April 2009 during the Iceberg III (IB 03) cruise. Stations were labeled by area: near C-18a and far C-18a are in western waters of the Powell Basin (0.3–1.0 km and 16–18 km away from C-18a iceberg, respectively), Iceberg Alley is towards the southern Powell Basin in an area with high concentration of icebergs (> 74 km away from C-18a) and the control site towards the mouth of the Powell Basin (74 km away from C-18a).

Area	Station	Latitude (°S)	Longitude (°W)	Date	Distance from iceberg (km)	Mixed Layer Depth (m)	Average Salinity	Average Temp. (°C)
Iceberg Alley	147	62.806	49.883	04/04/09	–	45	34.145	−1.097
	154	62.858	50.073	04/05/09	–	32	34.197	−1.185
near C-18a	3	62.256	51.689	03/10/09	0.58	56	34.028	−0.610
	29	61.967	51.352	03/16/09	0.49	51	33.995	−0.441
	39	62.793	51.599	03/17/09	0.71	25	34.100	−0.775
	101	62.369	50.713	03/29/09	0.32	32	34.239	−0.725
	108	61.481	50.318	03/30/09	0.72	50	34.119	−0.347
far C-18a	8	62.311	51.601	03/11/09	16.6	24	33.920	−0.460
	46	61.562	51.484	03/18/09	17.8	20	33.988	0.083
	56	61.500	51.520	03/20/09	18.5	40	34.111	−0.199
	65	61.512	51.618	03/20/09	18.0	n/a	34.150	−0.185
	121	61.446	50.638	04/01/09	17.8	40	34.133	−0.289
control site	141	61.687	48.636	04/03/09	74	55	33.913	0.023
	170	61.794	48.440	04/07/09	74	47	33.901	−0.089

Temperature and salinity data are averaged 0–100 m depth.

filtered through 0.2 μm membrane filters, extracted in 90% acetone and concentrations measured with a digital Turner Designs fluorometer model 10-AU. Calibration was performed with known amounts of chl *a* (Sigma Co) previously determined spectrophotometrically.

Differences between means in phytoplankton abundance, temperature and salinity in the different study areas were tested with Mann-Whitney test (Zar, 1996). Principal Component Analysis (PCA) was used to find relationships between the abundance of different phytoplankton taxa and water masses (as defined by temperature and salinity) in the different sampled areas. The taxa chosen for this analysis were: small diatoms (*Fragilariopsis nana* and *F. pseudonana*), larger diatoms (> 10 μm), dinoflagellates, cryptophytes, prasinophytes, silicoflagellates, and small flagellated and coccoid cells. Significance is presented at $\alpha=0.05$ and $\alpha=0.1$. Statistical software included Statistica 7.

3. Results

Waters of the Powell Basin, where this study was carried out, are located in the northwestern Weddell Sea. Icebergs travel in a north-northeast drift towards the Scotia Sea (Fig. 1). The two areas where the effect of icebergs on surface waters (0–~100 m depth) was studied included the southwestern Powell Basin, with numerous icebergs observed at the time of sampling (labeled Iceberg Alley), and C-18a, a tabular iceberg 35 km long and 6 km wide originating from the Ross Sea during a calving event in 2003 (Helly et al., 2011). After drifting counterclockwise around the Antarctic continent, it reached the western Powell Basin 6 years later (Smith, 2011).

3.1. Description of phytoplankton taxa

A total of fifty-eight taxa were found in this study (Table 2). The most abundant groups were diatoms and unidentified small flagellated and coccoid cells. Other groups, such as dinoflagellates, cryptophytes, prasinophytes and silicoflagellates were present in low concentration. In addition, a filamentous cyanobacterium was exceptionally found in a few samples. Ciliates and choanoflagellates were not analyzed although they were also present in almost all the samples. Identification of individual cells was performed to the lowest possible taxonomical level, i.e. most diatoms were identified to genus or species level. However, micro-flagellates and coccoid cells were too small to identify and they were lumped into the category "small flagellated and coccoid cells < 7 μm". We summarize the properties of the main taxa and compare their concentration in the four studied areas.

3.1.1. Diatoms

Diatoms were the numerically dominant group in most samples. *Fragilariopsis* was the best represented genus (*F. nana*, *F. pseudonana*, *F. curta*, *F. rhombica*/*separanda* and *F. obliquecostata* in order of importance within the genus). *F. nana* was observed as solitary cells or in doublets and *F. curta* appeared forming short ribbon-like colonies (Fig. 2A-E). During the cell counts we could not distinguish between *F. rhombica* and *F. separanda* due to their narrow similarity and they are cited as one taxon. *F. kerguelensis* was only found in net samples (Fig. 2F). Small centric diatoms, 9–18 μm in diameter, were also highly abundant. *Thalassiosira gracilis* var. *expecta*, *T. gracilis* var. *gracilis* and *T. perpusilla* were characteristic of this group (Fig. 2G-I). In addition other *Thalassiosira* species were found, generally as single cells. Typical centric taxa as *Actinocyclus actinochilus* (Fig. 2J), *Asteromphalus hookeri*, *A. parvulus* and *Coscinodiscus oculoides* were observed in smaller abundance, the latter (Fig. 2K), in a few samples. *Chaetoceros* was the genus with the highest species richness with ten species identified. *C. dichaeta* (Fig. 3A, B) and *C. curvatus* (Fig. 3C-E) were the most prominent ones, although all presented low density. *C. criophilus* (Fig. 3F) together with *Corethron pennatum* (Fig. 3G, H) appeared to be the dominant diatoms retained by the 20 μm mesh in the qualitative samples. *C. pennatum* was observed in different stages of reproduction (Fig. 3G). *Leptocylindrus mediterraneus* was a species easily identified by the presence of epiphytic flagellates fixed to the girdle bands (Fig. 3I-L). *Odontella weissflogii* and *Eucampia antarctica* (Fig. 4A, B) generally occurred forming short chains. *Pseudo-nitzschia* spp. and *Haslea* sp. (Fig. 4C-E) were well represented in all samples. *Pseudo-nitzschia* spp. were divided into two size categories: narrow (transapical axis was 1.4–1.7 μm) and broad (transapical axis was 3.0–5.5 μm), the narrowest ones tending to be shorter than the widest ones. Another diatom species was *Dactyliosolen tenuijunctus*, occurring normally as solitary cells (Fig. 4F, G).

3.1.2. Small flagellated and coccoid cells

We included in this group those unicellular naked organisms, more o less spherical, with size between 1.5 and 7 μm in

Table 2
Phytoplankton taxa identified during the cell counts in the four sampling areas. Abbreviations as in Table 1.

Taxa	Area			
	Iceberg Alley	near C-18a	far C-18a	control site
Diatoms				
Actinocyclus actinochilus (Ehrenberg) Simonsen*		+	+	+
Asteromphalus hookeri Ehrenberg		+	+	+
Asteromphalus parvulus Karsten		+	+	+
Chaetoceros aequatorialis Cleve	+	+	+	+
Chaetoceros atlanticus Cleve		+	+	+
Chaetoceros bulbosus (Ehrenberg) Heiden	+	+	+	+
Chaetoceros concavicornis Mangin	+	+	+	+
Chaetoceros convolutus Castracane	+	+	+	
Chaetoceros criophilus Castracane*	+	+	+	+
Chaetoceros curvatus Castracane	+	+	+	+
Chaetoceros dichaeta Ehrenberg*	+	+	+	+
Chaetoceros flexuosus Mangin		+		
Chaetoceros neglectus Karsten	+	+	+	+
Corethron pennatum (Grunow) Ostenfeld*	+	+	+	+
Coscinodiscus oculoides Karsten*		+	+	
Cylindrotheca closterium (Ehrenberg) Reimann & Lewin		+		
Dactyliosolen tenuijunctus (Manguin) Hasle	+	+	+	+
Eucampia antarctica var. *recta* (Mangin) Fryxell & Prasad		+	+	+
Fragilariopsis curta (van Heurck) Hustedt*	+	+	+	+
Fragilariopsis nana (Steemann Nielsen) Paasche*	+	+	+	+
Fragilariopsis obliquecostata (van Heurck) Heiden*	+	+		
Fragilariopsis pseudonana (Hasle) Hasle*	+	+	+	+
*Fragilariopsis rhombica/separanda**	+	+	+	+
Haslea sp.*	+	+	+	+
Leptocylindrus mediterraneus (Peragallo) Hasle*		+	+	+
Membraneis challengeri (Grunow) Paddock	+	+	+	+
Navicula sp.		+	+	
Nitzschia sp.		+		
Odontella weissfloguii (Grunow) Grunow		+	+	
Plagiotropis gaussii (Heiden in Heiden & Kolbe) Paddock	+	+	+	+
Proboscia inermis (Castracane) Jordan & Ligowski*	+	+	+	+
Proboscia truncata (Karsten) Nöthig & Ligowski	+	+	+	+
Pseudo-nitzschia spp. (narrow)*	+	+	+	+
Pseudo-nitzschia spp. (broad)*	+	+	+	+
Rhizosolenia sp.			+	
Stellarima microtrias (Ehrenberg) Hasle & Sims	+	+	+	+
Thalassiosira gracilis (Karsten) Hustedt var. gracilis*	+	+	+	+
Thalassiosira gracilis var. *expecta* (VanLandingham) Fryxell & Hasle	+	+	+	+
Thalassiosira perpusilla Kozlova	+	+	+	+
Thalassiothrix antarctica Schimper ex Karsten		+	+	+
cf. *Manguinea* sp.		+	+	+
non identified Centrales*	+	+	+	+
non identified Pennales		+	+	+
Small flagellated and coccoid cells <7 µm				
Flagellated and coccoid cells	+	+	+	+
Cryptophytes				
Cryptomonas spp.	+	+	+	+
Prasinophytes				
Pyramimonas cf. *tychotreta*	+	+	+	+
Dinoflagellates				
Alexandrium sp.			+	
Amphidinium hadai Balech	+	+	+	+
Gonyaulax sp.		+		
Gymnodinium spp.	+	+	+	+
Gyrodinium lachryma (Meunier) Kofoid & Swezy	+	+	+	+
Gyrodinium spp.	+	+	+	+
Preperidinium cf. *perlatum*	+		+	
Prorocentrum sp.	+			
Protoperidinium spp.		+	+	+
Silicoflagellates				
Dictyocha speculum Ehrenberg*	+	+	+	+
Cyanobacteria				
cf. *Anabaena* sp.			+	+
Prymnesiophytes				
Colonial *Phaeocystis* sp.		+	+	
Total number of taxa at each area:	37*	53	52	44
Total number of diatoms taxa at each area:	27	42	39	34

(*) indicate taxa present in the Lagrangian sediment trap material collected under C-18a and in the control site (Smith et al., 2011).
(**) and (*) indicate area with significantly different number of taxa from near C-18a iceberg (<1 km) at $p<0.05$ and $p<0.10$, respectively.

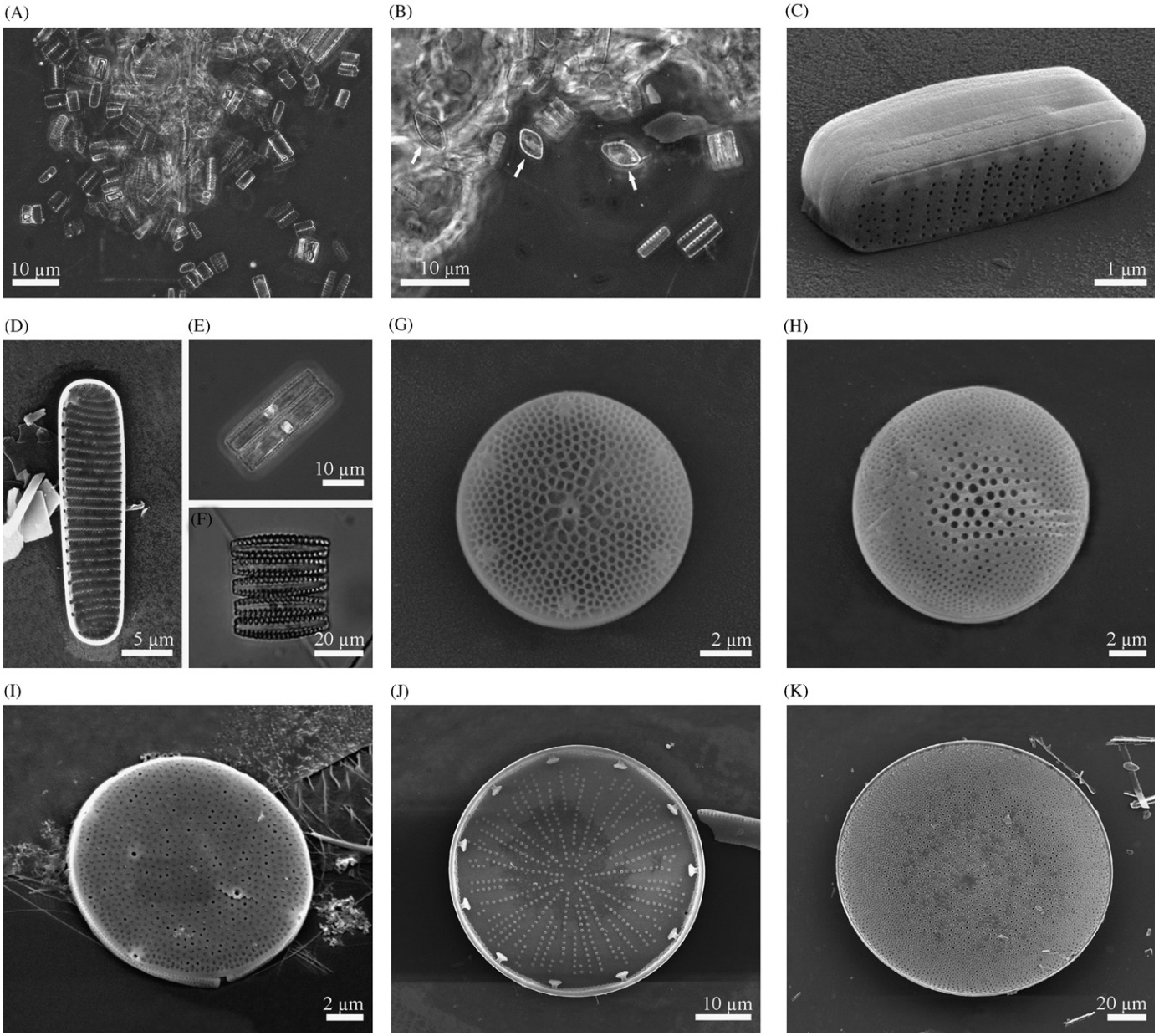

Fig. 2. A, LM Cells of *Fragilariopsis nana* abundant in the samples. B, LM Cells of *F. nana* and *F. pseudonana* (see arrows). C, SEM Frustule of *F. nana* shown in valve and girdle view. D, SEM Valve of *F. curta* in internal view. E, LM Cells of *F. curta* in short ribbon-like colony. F, LM Cells of *F. kerguelensis* in ribbon-like colony. G, SEM Valve of *Thalassiosira gracilis* var. *expecta* in external view. H, SEM Valve of *T. gracilis* var. *gracilis* in external view. I, SEM Valve of *T. perpusilla* in external view. J, SEM Valve of *Actinocyclus actinochilus* in internal view. K, SEM Valve of *Coscinodiscus oculoides* in internal view.

diameter. Some of these cells were characterized by the presence of one long and coil flagella. A reliable recognition of these small organisms requires culture studies and analysis with electron microscope. More of them belong probably to cryptophytes and prasinophytes, but as additional studies were not possible; we are unable to give a precise identification of them.

3.1.3. Cryptophytes and prasinophytes

Cryptomonas spp. were distinguished by their asymmetrical cell shape, dorsiventrally constructed, and by their two flagella with subapical insertion (Fig. 4H). The *Cryptomonas* size varied from 8.5 to 13.0 µm long. *Pyramimonas* cf. *tychotreta* was identified by the pyramidoidal cell shape, the presence of four flagella slightly longer than the cell body and by a basal pyrenoid (Fig. 4I). The size of the cells was ca. 6.5 µm long.

3.1.4. Dinoflagellates

Gyrodinium and *Gymnodinium sensu lato* were the most conspicuous dinoflagellate genera. Both are unarmored and in our material they occurred as single cells and in general in small size (Fig. 4J-L). It is difficult to differentiate one genus from the other; the cingulum displacement has been used to distinguish them. *Gyrodinium* would have the cingulum displaced more than one-fifth of the cell length, whereas *Gymnodinium* would have it displaced less than one-fifth or in equatorial position (Steidinger and Tangen, 1997; Mc Minn and Scott, 2005). On the other hand, *Gyrodinium lachryma* could be easily recognized by its teardrop shape and size. The organisms identified as *Gyrodinium* spp. measured between 13 and 98 µm and the ones as *Gymnodinium* spp. between 9 and 36 µm. *Amphidinium hadai* was another numerically well represented unarmored dinoflagellate. Armored dinoflagellates were also found but in low concentration, among

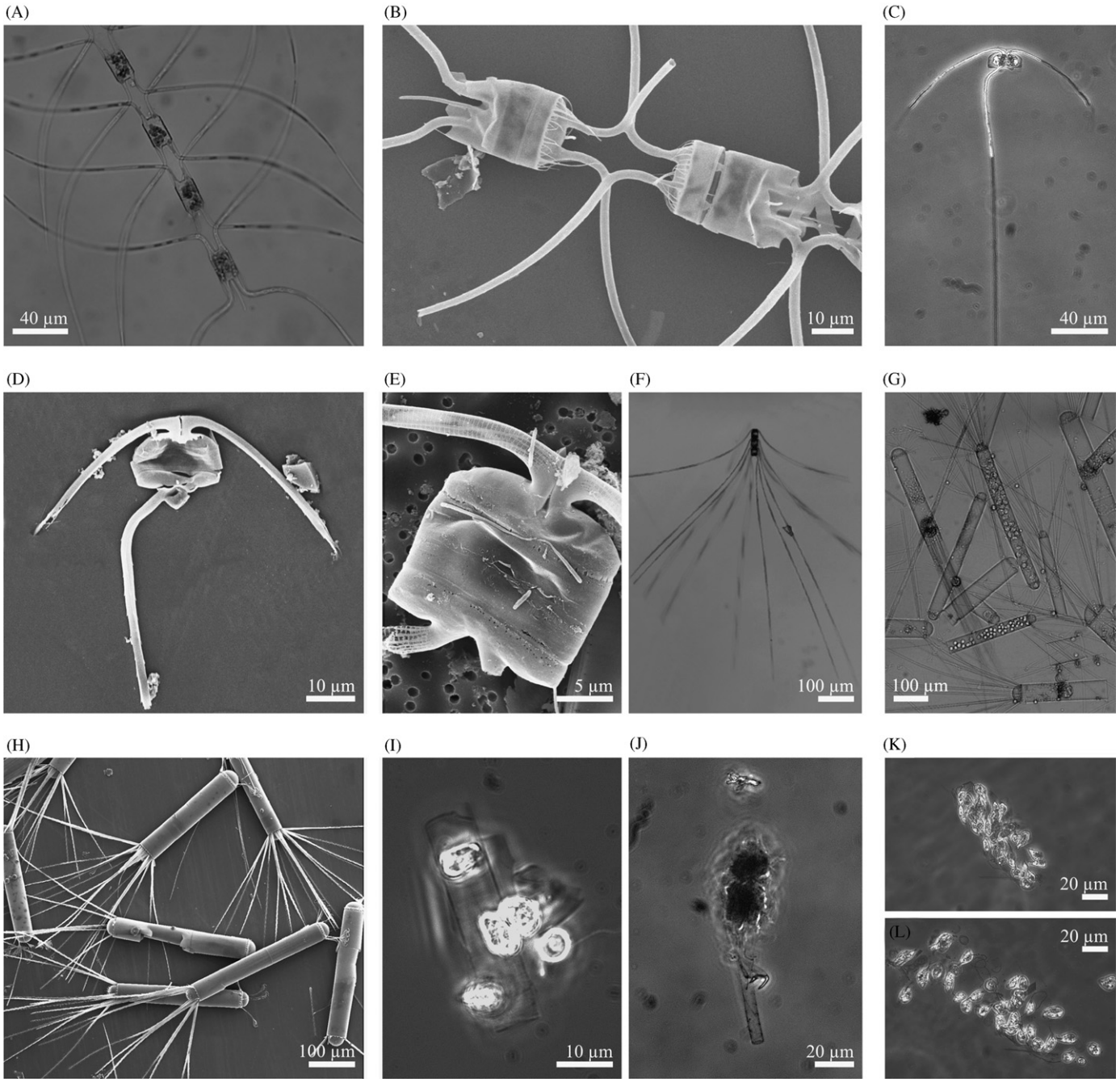

Fig. 3. A, B, LM and SEM, respectively, cells of *Chaetoceros dichaeta* in chain. C, LM Solitary cell of *C. curvatus*. Note the presence of chloroplasts in the setae. D, SEM Solitary frustule of *C. curvatus*. Note the setae armed with spines. E, SEM Detail of the frustule of *C. curvatus*. Note the origin point of setae, both located in the center of each valve, as well as its delicate ornamentation. F, LM Cells of *C. criophilus* in chain. G, LM Cells of *Corethron pennatum*. Note the presence of spermatogonangia containing spermatogonia. H, SEM General view of *C. pennatum*. I-K, LM empty frustules of *Leptocylindrus mediterraneus* with different degrees of epiphyte *Solenicola setigera* coverage. L, LM Cells of *Solenicola setigera* disaggregated by mechanical action.

them *Preperidinium* cf. *perlatum*, *Prorocentrum* sp. and *Protoperidinium* spp. *Dinophysis antarctica* was only found in net samples (Fig. 4M).

3.1.5. Silicoflagellates

Dictyocha speculum was easily identified; this species is characterized by its hexagonal siliceous skeleton composed by two hexagonal rings, one larger than the other, and linked by six bars. Six long spines also protruded from the largest ring (Fig. 4N, O). Although we did not find them, unarmored stages may also be present.

3.1.6. Cyanobacterium

A filamentous blue-green alga was found in a few samples (Fig. 4P, Q). Although it appears to be an *Anabaena* sp. we could not see heterocysts for a more reliable identification.

3.2. Hydrology of the region

The physical properties of the water column, in particular those within the mixed layer, where most of the phytoplankton biomass was found (Vernet et al., 2011), were characterized by their temperature and salinity (Fig. 5). Waters of the

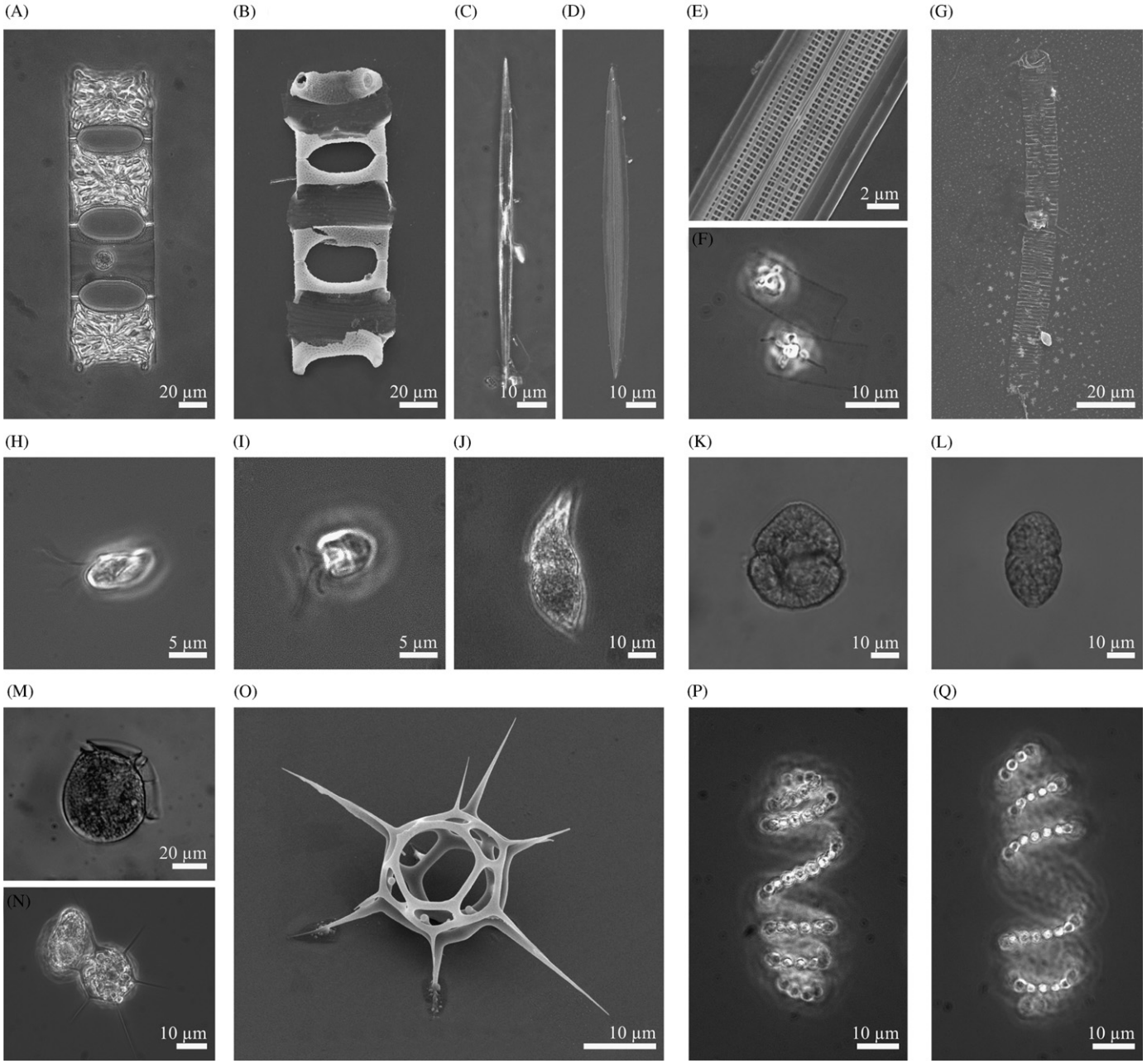

Fig. 4. A, B, LM and SEM, respectively, cells of *Eucampia antarctica* var. *recta* in straight chains shown in broad girdle view. C, D, LM and SEM, respectively, cells of *Haslea* sp. in valve view. E, Part of valve of *Haslea* sp. showing the striae in detail. F, LM Cells of *Dactyliosolen tenuijunctus*. Note its prominent and central nucleus. G, SEM Frustule of *D. tenuijunctus* lightly silicified. H, LM Cell of *Cryptomonas* sp. I, LM Cell of *Pyramimonas* cf. *tychotreta*. Note its basal pyrenoid. J, LM Cell of *Gyrodinium* sp. K, L, LM Cells of *Gymnodinium* sp. M, LM Cell of *Dinophysis antarctica*. N, LM Cell of *Dictyocha speculum*. O, SEM Skeleton of *D. speculum* of cell undergoing division. P, Q, LM Filamentous blue-green alga cf. *Anabaena* sp.

Iceberg Alley were cold and saline, ($\bar{x}=-1.031\pm0.197$ °C and $\bar{x}=34.049\pm0.149$, respectively) within the mixed layer (ML, surface~40 m) (Table 1 and 3). The highest average temperature and lowest salinity occurred at the control site with $\bar{x}=0.173\pm0.010$ °C and $\bar{x}=33.831\pm0.001$, respectively; temperatures at 25 and 40 m depth were significantly different from near IB C-18a ($p<0.1$). Waters affected by the iceberg C-18a also had low average temperatures and relatively high salinities at the ML ($\bar{x}=-0.302\pm0.276$ °C and $\bar{x}=33.991\pm0.058$, respectively), although not as cold as in Iceberg Alley. In contrast, water properties 18 km away from C-18a (far C-18a) were more similar to the control ($\bar{x}=0.081\pm0.186$ °C and $\bar{x}=33.955\pm0.053$). These observations indicate a decreasing gradient in phytoplankton composition and abundance along decreasing temperatures, from the control site, to far C-18a, to near C-18a and finally to Iceberg Alley (Fig. 5 and Table 3).

3.3. Phytoplankton distribution

The species composition was similar in all studied areas in the Powell Basin. Variability was observed in the number of taxa with 53 and 52 identified in near C-18a and far C-18a respectively, 44 in the control site and 37 in Iceberg Alley (Table 2). The number of taxa per area was significantly lower at Iceberg Alley ($p<0.1$). Of a total possible 58 taxa, 33 of them were common to all sampling areas.

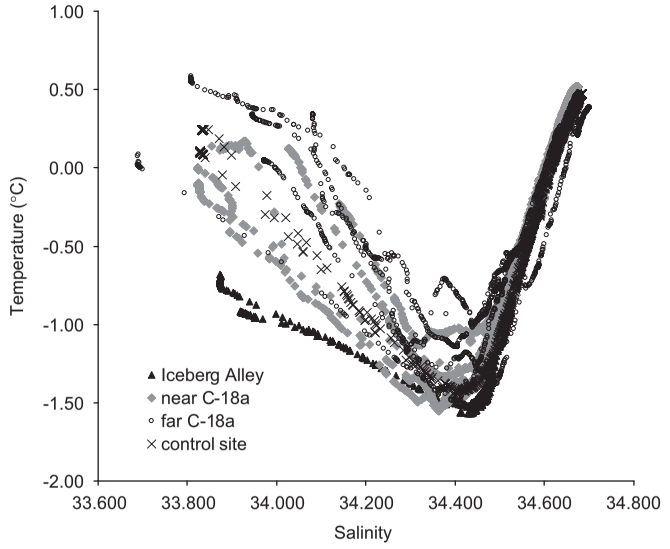

Fig. 5. Temperature and Salinity (T-S) relationships, 0–500 m depth, in the four sampled areas: Iceberg Alley (black triangles), near C-18a (gray rhombus), far C-18a (circles) and the control site (crosses). The temperature minimum is at ~100 m depth; seasonal mixed layer is indicated by fresher and warmer waters and the permanent thermocline by more saline and warmer waters.

Table 3
Physical properties in the four areas studied corresponding to the depth of phytoplankton sampling. Results are expressed as average per depth per area. Abbreviations as in Table 1.

Area	Depth (m)	Salinity	Temperature (°C)
		Average	
Iceberg Alley	**surface**	33.903	−0.843 (*)
	~25	34.043	−1.014 (*)
	~40	34.202	−1.236 (*)
	~100	34.486 (*)	−1.304
near C-18a	**surface**	33.930	−0.015
	~25	34.000	−0.325
	~40	34.045	−0.565
	~100	34.363	−1.277
far C-18a	**surface**	33.906	0.260
	~25	33.948	0.093 (**)
	~40	34.012	−0.111
	~100	34.374	−1.187
control site	**surface**	33.830	0.185
	~25	33.831	0.169 (*)
	~40	33.833	0.165 (*)
	~100	34.345	−1.325

(**) and (*) indicate depths with significantly different properties from the waters near C-18a iceberg (< 1 km) at $p < 0.05$ and $p < 0.10$, respectively.

3.3.1. Spatial variability

Total phytoplankton abundance varied considerably by depth and among the four studied areas (near C-18a, far C-18a, Iceberg Alley and control site, Table 4). The values ranged from a minimum of 39,923 cells l^{-1} at 100 m depth at Iceberg Alley to a maximum of 2,402,635 cells l^{-1} at 26 m depth at the control site. Usually the highest concentrations were found in surface waters (nine out of 14 stations) and the lowest ones at ~100 m depth at all stations.

In the mixed layer total phytoplankton density was lower at Iceberg Alley than in the other three areas (surface—~40 m layer, $\bar{x}$=311,477 cells l^{-1}), middle values were recorded at near C-18a and far C-18a ($\bar{x}$=753,816 and 760,341 cells l^{-1}, respectively), and the highest ones were found at the control site

Table 4
Phytoplankton abundance in the four sampling areas. Microscopic analyses were combined into six main groups. Results are expressed as average per depth per area. Abbreviations as in Table 1.

Area	Depth (m)	Total Phytoplankton	Diatoms	Small flagellated and coccoid cells < 7 µm	Cryptophytes	Prasinophytes	Dinoflagellates	Silicoflagellates
		Average ± standard deviation in cells l^{-1}						
Iceberg Alley	**surface**	380,871 ± 85,047	184,708 ± 20,249	134,593 ± 76,947	17,183 ± 8,100	14,319 ± 2,024	20,762 ± 1,013	16 ± 8 (*)
	~25	304,804 ± 77,201	160,367 ± 38,474	100,587 ± 29,868 (*)	6,801 ± 506 (*)	2,864 ± 2,025	26,131 ± 9,618	0
	~40	248,758 ± 76,911	78,394 ± 47,080	137,227 ± 19,417	4,679 ± 2,061 (*)	1,151 ± 108 (*)	14,958 ± 1,411	5 ± 7 (*)
	~100	49,386 ± 13,383 (*)	4,700 ± 3,073 (*)	35,375 ± 10,720	1,150 ± 197	935 ± 107	5,218 ± 1,912	88 ± 51
near C-18a	**surface**	905,928 ± 384,377	664,089 ± 399,233	156,858 ± 32,235	28,279 ± 9,784	7,947 ± 8,093	23,267 ± 6,200	80 ± 44
	~25	906,337 ± 574,023	625,266 ± 519,978	199,701 ± 44,666	25,630 ± 14,358	4,950 ± 5,339	29,455 ± 23,931	56 ± 37
	~40	449,182 ± 345,013	292,573 ± 283,549	103,761 ± 55,988	14,235 ± 7,833	4,880 ± 2,733	18,005 ± 7,132	76 ± 34
	~100	98,468 ± 14,532	22,778 ± 3,549	56,385 ± 15,115	5,381 ± 3,378	1,677 ± 1,058	7,409 ± 1,747	130 ± 92
far C-18a	**surface**	921,964 ± 464,855	550,687 ± 414,466	273,053 ± 78,388 (**)	37,801 ± 22,040	11,168 ± 5,513	18,184 ± 11,814	93 ± 37
	~25	774,865 ± 301,791	438,279 ± 254,222	225,135 ± 48,390	40,133 ± 29,903	12,739 ± 7,099 (*)	36,966 ± 18,142	116 ± 72
	~40	584,192 ± 209,839	311,512 ± 186,048	180,069 ± 22,375 (*)	34,847 ± 22,015	7,045 ± 8,333	28,952 ± 20,012	165 ± 145
	~100	88,241 ± 35,505	15,703 ± 7,296 (*)	53,241 ± 25,641	3,528 ± 2,125	1,348 ± 1,109	7,488 ± 2,353	147 ± 182
control site	**surface**	1,696,736 ± 739,101	1,344,502 ± 654,053	230,527 ± 42,524 (*)	47,251 ± 22,274	2,864 ± 0	31,501 ± 0 (*)	26 ± 37
	~25	2,130,585 ± 384,738 (*)	1,828,466 ± 370,563 (*)	174,685 ± 24,299	64,433 ± 22,274 (*)	0	28,637 ± 8,099	31 ± 14
	~40	1,696,736 ± 204,519 (*)	1,470,504 ± 151,870 (*)	114,548 ± 32,399	55,842 ± 10,124 (*)	0 (*)	32,933 ± 10,125	26 ± 22
	~100	70,652 ± 2,140 (*)	18,573 ± 4,397	38,854 ± 5,193	2,547 ± 1,866	624 ± 274 (*)	6,075 ± 86	129 ± 37

(**) and (*) indicate depths with significantly different results from the waters near C-18a iceberg (< 1 km) at $p < 0.05$ and $p < 0.10$, respectively.

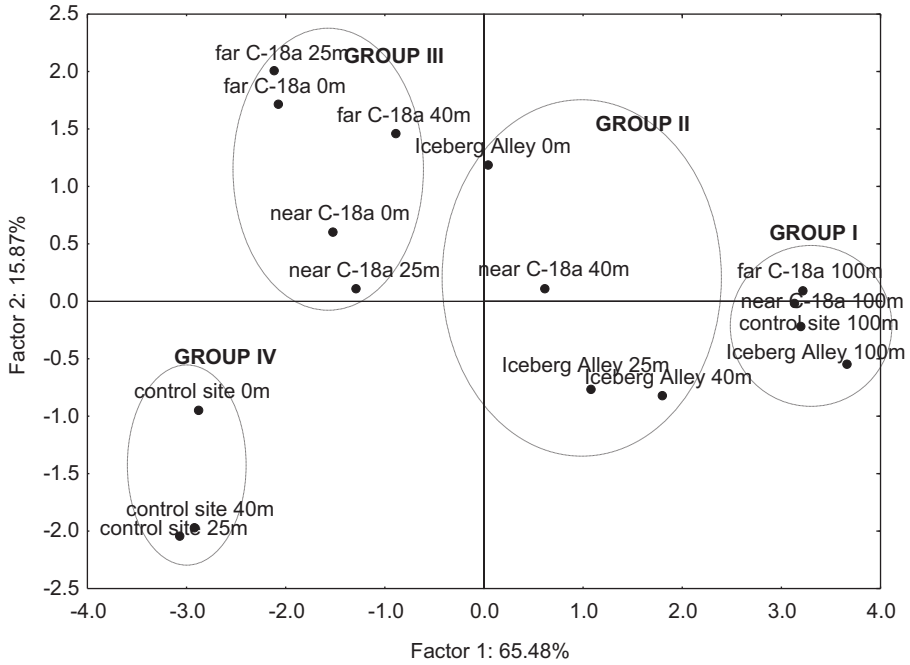

Fig. 6. Results from the Principal Component Analysis (PCA) using average abundance of seven phytoplankton groups, temperature and salinity as variables. Group I to IV are identified along the first component, along an increasing temperature gradient.

Table 5
Eigenvectors estimated with the Principal Component Analysis showing the correlation of each variable with the first three factors.

Eigenvectors of correlation matrix			
Variable	**Factor 1**	**Factor 2**	**Factor 3**
Small diatoms	−0.34023	−0.42066	0.17307
Large diatoms	−0.36389	0.02368	0.29728
Small flagellated and coccoid cells	−0.34377	0.29650	−0.11066
Dinoflagellates	−0.36570	0.01369	−0.14712
Cryptophytes	−0.38610	−0.13588	0.22526
Prasinophytes	−0.14306	0.71277	−0.32236
Silicoflagellates	0.13793	0.44734	0.77408
Temperature	−0.39744	0.08718	0.20291
Salinity	0.39165	−0.01307	0.22968

($\bar{x}$=1,841,352 cells l^{-1}, $p<0.1$). A different pattern was observed at ~100 m depth, where the highest concentrations were at C-18a areas ($\bar{x}$=88,241 and 98,468 cells l^{-1} at far C-18a and near C-18a, respectively, $p<0.1$) and the middle values were at the control site ($\bar{x}$=70,652 cells l^{-1}) (Table 4).

Diatoms were the dominant group within the mixed layer or upper 40 m of the water column (105,956–2,090,493 cells l^{-1}, Table 4). Average diatom concentration was lower at Iceberg Alley than in the other areas at the surface—~40 m layer ($\bar{x}$=141,156 cells l^{-1}) and its contribution to total phytoplankton was also the lowest (45.32%). The average values were 433,493 at far C-18a, 527,310 at near C-18a and 1,547,824 cells l^{-1} at the control site, with a contribution to total phytoplankton of 57.01%, 69.95% and 84.06%, respectively. Compared to near C-18a, diatoms concentrations at ~25 and 40 m depth were significantly different from the control site ($p<0.05$). In waters around the C-18a iceberg, average diatom density was 21.64% higher at near C-18a than at far C-18a. At ~100 m depth, diatoms were significantly higher at near C-18a ($\bar{x}$=22,778 cells l^{-1}, $p<0.1$), as represented by *Fragilariopsis nana* distribution, high at the control site ($\bar{x}$=18,573 cells l^{-1}), intermediate at far C-18a ($\bar{x}$=15,703 cells l^{-1}), and lower at Iceberg Alley ($\bar{x}$=4700 cells l^{-1}).

F. nana was the most prominent taxon, representing 56.67% and 82.26% of total phytoplankton and diatom density, respectively. Due to its small size, its contribution to total phytoplankton biomass, expressed as μg chl *a* l^{-1}, was only 9.12%. In the surface—~40 m layer the total chl *a* concentration, as a measure of phytoplankton biomass, varied from 0.1365 (at 34 m depth, station 147—Iceberg Alley) to 0.7246 μg l^{-1} (at surface, station 65-far C-18a) while the contribution by *F. nana*, obtained through cell volume calculation, varied from 1.3% to 22.9% of the total: 0.0022 μg l^{-1} at 50 m depth, station 101-near C-18a to 0.0910 μg l^{-1} at 26 m depth, station 141-control site.

Small flagellated and coccoid cells dominated at ~100 m depth (22,766–83,047 cells l^{-1}), at all depths in some occasions (stations 101 and 65, near and far C-18a, respectively) as well as at 34 and 36 m depth at stations 147 and 154-Iceberg Alley, respectively. With regard to small flagellated and coccoid cells at surface—~40 m, the higher values were registered at far C-18a, significantly higher than at near C-18a (47.34%), showing on average 226,085 cells l^{-1} with significant difference at surface ($p<0.05$) and at the base of the mixed layer (~40 m, $p<0.1$, Table 4).

With regard to the non-dominant groups, cryptophytes showed the highest and the lowest densities in the mixed layer at the control site and at Iceberg Alley, respectively ($\bar{x}$=55,842 and 9554 cells l^{-1}) with significant differences at ~25 and 40 m depth in both areas ($p<0.1$, Table 4). In contrast, prasinophytes presented the lowest values of abundance at the control site at all depth. Dinoflagellates showed different patterns of concentrations; however its relative abundance increased with depth. The silicoflagellate *Dictyocha speculum* showed a greater average concentration at far C-18a and at near C-18a than at the other two areas, and in general, the highest densities occurred at ~100 m depth (maximum concentration of 454 cells l^{-1} at 125 m depth, station 8-far C-18a). Considering only waters around the C-18a iceberg, silicoflagellates, prasinophytes,

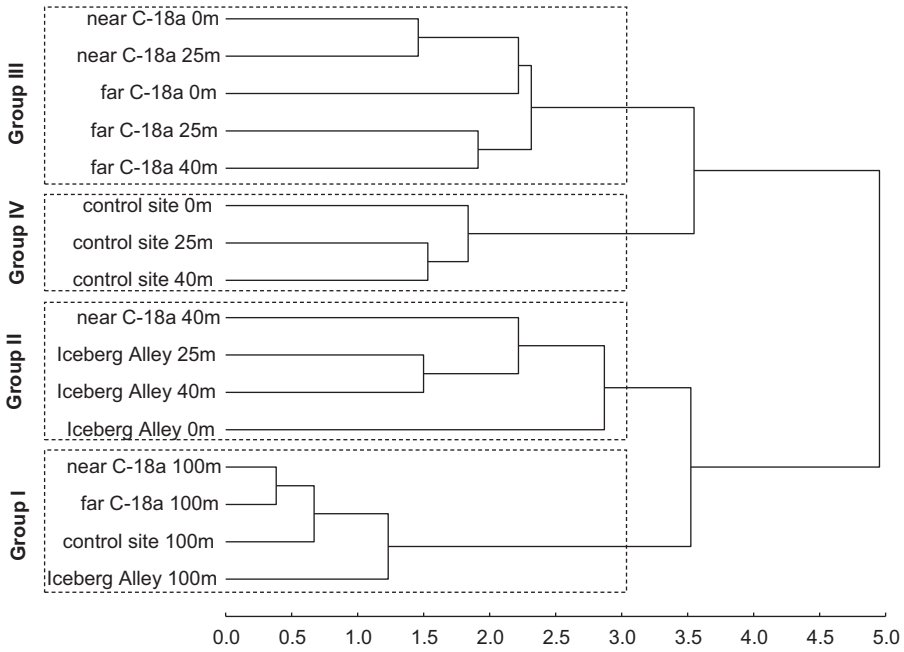

Fig. 7. Cluster of areas using average abundance of seven different phytoplankton groups, temperature and salinity as variables, with Euclidean distances and Unweighted pair-group averages as grouping method.

cryptophytes and dinoflagellates were 76.42%, 74.11%, 65.50% and 18.91% higher at far C-18a than at near C-18a at the same depth (0—~40 m); except for prasinophytes (Table 4), these differences were not significant. At 100 m depth the trend was reversed for cryptophytes and prasinophytes, with 52.52% and 24.41% higher abundance near the iceberg.

3.3.2. Phytoplankton distribution in relation to environmental factors

The Principal Component Analysis determined three major components explaining 65.48, 15.87 and 10.79% of the total variability, respectively (Fig. 6). The first component was significantly correlated with seven out of the nine variables: cryptophytes, dinoflagellates, large diatoms, small diatoms, small flagellated and coccoid cells, salinity and temperature (except salinity, all of them were negatively correlated). The second component was significantly correlated with prasinophytes and moderately correlated with silicoflagellates and small diatoms (the latter, negatively) (Table 5).

The graphical representation (Fig. 6) and the cluster (Fig. 7) constructed from the first two principal components show similar results. We infer from those, four groups: 1) Group I, includes all samples from ~100 m depth. 2) Group II, defined by samples from surface—~40 m layer at Iceberg Alley and ~40 m depth at near C-18a. 3) Group III, includes the surface—~40 m layer samples at C-18a, near and far, with the exception of ~40 m depth at near C-18a. 4) Group IV, formed by samples from the surface—~40 m layer at the control site. The first component distinguishes a gradient of abundance of the different phytoplankton taxa (except prasinophytes and silicoflagellates) that increases from Group I to Groups II, III and IV according to their relevance, along a gradient of increasing temperature and, to a lesser extent, decreasing salinity (Fig. 6). Group I differentiates deep samples at the depth of temperature minimum. The other three groups include mixed-layer depth samples (surface—~40 m). Lowest temperature are combined with lowest cell abundance at Iceberg Alley, highest temperature waters with highest cell abundance at the control site and intermediate phytoplankton abundance for the C-18a areas, colder for near C-18a and warmer for far C-18a. Some near C-18a samples were closer to Iceberg Alley, such as ~40 m depth in near C-18a that is included in Group II (Fig. 7). The PCA also shows a slight gradient of phytoplankton abundance within the Group III, lower from ~40 m at far C-18a, to ~25 m at near C-18a, to 0 m at near C-18a, to 0 m at far C-18a to ~25 m at far C-18a. Similarly, in Group I (all locations at ~100 m depth) the analysis reflects somewhat higher phytoplankton abundance in near C-18a than in far C-18a. The second component reflects a higher abundance of prasinophytes in Group III and in Iceberg Alley at 0 m depth than in the other Groups. In summary, this analysis suggests lower phytoplankton density at the mixed layer associated with conditions of lower water temperatures; these conditions are prevalent in areas affected by icebergs, Iceberg Alley with many small and medium icebergs and near C-18a near one large iceberg.

4. Discussion

Antarctic phytoplankton is habitually dominated by diatoms in areas of high productivity; however, high contributions of other taxonomic groups often occur (Estrada and Delgado, 1990). Spatial and temporal variability in abundance and relative concentrations of the different taxa are reported for coastal and oceanic waters (e.g., Garibotti et al., 2003). This variability is likely related to the changing environmental characteristics of water masses, which create favorable conditions for different groups of organisms (Bianchi et al., 1992). Wind, sea ice cover and meltwater, or freshwater input from glaciers, strength of upwelling, mesoscale eddies, fronts and variation in currents, are some examples of sources of changes in the Antarctic waters characteristics (Smith and Nelson, 1985; Kopczynska, 1988; Villafane et al., 1995; Coale et al., 2004; Boyd et al., 2007). Superimposed to physical and chemical changes we can expect biological processes, such as zooplankton grazing, to modify the abundance and dominance of different taxonomic assemblages (Knox, 2007). Here we present evidence that icebergs can also affect phytoplankton composition and abundance in surrounding waters at a local and regional scale and that the changes are consistent with

meltwater distribution. Furthermore, top-down control of phytoplankton abundance from zooplankton assemblages associated with the iceberg could be significant.

4.1. Taxonomic composition

The taxonomic composition of the phytoplankton communities showed similarity among the four studied areas of the Powell Basin, in the northwestern Weddell Sea. From a total of 58 taxa found, 18 were identified in the sediment trap material collected under iceberg C-18a and at the control site (Smith et al., 2011). Diatoms and silicoflagellates, or the highly silicified species, were the main contributors to sedimenting matter and they are indicated with an asterisk (*) in Table 2.

Diatoms and among them *Fragilariopsis nana* dominated numerically at surface-~40 m in most stations. *F. pseudonana* and *F. curta* were also numerically important diatoms. Our results about the presence and abundance of *F. nana* are consistent with previous studies in the Weddell Sea (Kang and Fryxell, 1992, 1993; Socal et al., 1997; Lizotte, 2001) taking into account that our results could be comparable with those attributed to *F. cylindrus* in other studies (see below). *F. nana* is a marine planktonic and ice bipolar species of small size (2.4–15.5 μm long and 1.4–2.4 μm wide) recently typified by Lundholm and Hasle (2008) from material initially regarded as *F. cylindrus*. Due to the narrow similarity between *F. nana sensu stricto* and *F. cylindrus*, specimens previously referred to the latter would have corresponded to the former species (Lundholm and Hasle, 2008). The morphological characters that distinguish these two species can overlap; *F. nana* is mainly differentiated from *F. cylindrus* by a smaller valve width and a higher density of poroids (Lundholm and Hasle, 2008; Cefarelli et al., 2010). For this work we confirmed *F. nana* identification by Scanning Electron Microscope (SEM). After reviewing measurements and SEM micrographs in previous studies, we agree with Lundholm and Hasle's conclusions mentioned above.

The *Fragilariopsis* genus is well represented in Antarctica (Hasle and Medlin, 1990; Round et al., 1990; Cefarelli et al., 2010) and numerous studies (Kang and Fryxell, 1992, 1993; Socal et al., 1997; Hegseth and von Quillfeldt, 2002) show that populations of *Fragilariopsis* species can dominate phytoplankton and particularly diatom assemblages in sea ice and in the water column, particularly at the ice edge. El-Sayed and Fryxell (1993) suggested that *F. curta*, *F. cylindrus* and *Phaeocystis* are frequently dominant under sea ice as well as in coastal waters, and that due to their small size they could easily be undersampled. The widespread distribution of *Fragilariopsis* spp. in Antarctica is attributed to their tolerance to a wide range of environmental conditions. For example, *F. cylindrus* which is found as a dominant or co-dominant species in ice samples (Lizotte, 2001), is considered a species with a competitive advantage capable to grow under extreme conditions (depletion of dissolved inorganic carbon, oxygen oversaturation, alkaline pH) in sea ice (Gleitz et al., 1996; Lizotte, 2001). Furthermore, Garrison et al. (1987) reported a close similarity between the more frequent and abundant species found both in sea ice and water column, with *F. cylindrus* and *Phaeocystis pouchetii* (prymnesiophyte) as dominant taxa.

The identified *Thalassiosira* species (Fig. 2G-I), most of them as single cells, are known to have a widespread distribution in the Weddell Sea. In the northwestern Weddell Sea during spring, at the transition from the marginal ice zone to open water, Bianchi et al. (1992) found centric diatoms in large colonies dominating the phytoplankton assemblage, principally *Thalassiosira gravida* and *Chaetoceros neglectus*. Fryxell (1989) reported *Thalassiosira* species with multiple central strutted processes forming long chains through central threads. She found gelatinous colony formation of *T. gravida* and pointed the differences in growth habit and abundance of the same genus during autumn, when only a few specimens were recorded and *T. australis* occurred forming resting spores. Although we did not find *Thalassiosira* species in long chains, we did not find resting spores either, as expected if growth conditions had been unfavorable (Hasle and Syvertsen, 1997). *Coscinodiscus oculoides* observed in the C-18a areas, has been reported near King George Island and in the southern Weddell Sea (Ferrario et al., 2008).

Chaetoceros, the genus with the highest species richness in this study, is almost exclusively a marine diatom with high species diversity and distribution in neritic and oceanic waters (Hasle and Syvertsen, 1997; Rines and Hargraves, 1988). Most of these species appear forming chain colonies and only a few as single cells (Sunesen et al., 2008). We found *C. aequatorialis* and *C. curvatus* as solitary; being the latter one of the best represented species among the genus in our samples. *C. curvatus* is little known and a poorly reported taxon, recently described and illustrated by Scott and Thomas (2005). We could easily identify it with light microscopy by the setae point of origin, both placed in the center of each valve. *C. criophilus* and *Corethron pennatum* were the most prominent taxa in net plankton (cells > 20 um). We agree with Fryxell and Hasle (1971) and Fryxell (1989) who suggested that *Corethron* abundance has probably been overestimated when only nets have been used for sampling as their size and shape increases their retention. *C. pennatum* was frequently found as dividing cells as well as spermatogonangia containing spermatogonia in different numbers and, to a lesser degree, this specie was found in auxospore formation. Sometimes we also observed free spermatogonia. According with Crawford et al. (1998), it is worth noting that we use the name *Corethron pennatum* (Grunow) Ostenfeld in place of the old combination *Corethron criophilum* Castracane. In Antarctica, the recognized *Haslea* species is *H. trompii* (Hasle and Syvertsen, 1997; Scott and Thomas, 2005) but the specimens found by us differed from it with respect to the measure of the transapical axis and the number of transverse striae in 10 μm (5–9 μm wide and 25–26 striae in 10 μm in our material, 10–14 μm wide and 28–30 striae in 10 μm in the bibliography). Consequently, we could not identify this taxon at species level.

Leptocylindrus mediterraneus has a cylindrical shape with numerous girdle bands and can appear solitary or united by the valve face forming chains (Scott and Thomas, 2005). This species has a marine cosmopolitan distribution; in general it has been found without chloroplasts and with epiphytic flagellates attached to the girdle bands. On the other hand, its taxonomic position is questionable (Hasle and Syvertsen, 1997). According to Fryxell (1989) *L. mediterraneus* is frequently found in Antarctica, even under the ice and particularly it was well represented in deep waters in the Weddell Sea. While Scott and Thomas (2005) recognize the epiphytic flagellate as *Rhizomonas setigera*, Gómez (2007) prefers to retain *Solenicola setigera* name and call the association between both species consortium *Solenicola-Leptocylindrus*. *S. setigera*, only found living attached to the same empty diatom frustules, is a colonial protozoan that captures pico and small nano planktonic microalgae (Gómez, 2007). He reports different shapes, positions and degrees of *S. setigera* coverage on *L. mediterraneus*. This author also mentions the presence in some colonies of motile flagellum-like structures forming a tube covered by a tuft of hair-like structures. We confirmed different degrees of epiphyte coverage on *L. mediterraneus*, even entire frustules, and in some cases, the presence of hair-like structures (Fig. 3I-L). Across the Pacific Ocean (between 41°N and 34°S) Gómez (2007) found in eutrophic waters high consortium *Solenicola-Leptocylindrus* densities (1600 to 8000 frustules l^{-1}) forming long chains of frustules covered by a high percentage of

S. setigera. In these conditions, the density of large phytoplankton was lower than the one of picoplankton, suggesting that the latter could be part of the diet of *S. setigera*. In contrast, in oligotrophic waters the consortium abundance did not exceed 20 frustules l^{-1} and the highest abundance was at 100–150 m depth, below the subsurface chlorophyll maximum, where the presence of picoplankton would be also higher. Moreover, he mentions that the consortium was almost absent in surface waters during one transect. Considering our sampling sites with higher picoplankton relative abundance at greater depth, our values ranged from 10 to 72 frustules l^{-1} at C-18a at ~25–100 m layer and 31 frustules l^{-1} at the control site at 85 m depth. In agreement with Gomez (2007), we did not find *L. mediterraneus* in surface waters nor as long chains. The diameter of the frustules was shorter (5.10–8.80 μm) than that described in 1997 by Hasle and Syvertsen (7–35 μm). The measure of epiphytic flagellates ranged from 9 to 18 μm long and their shape was like a drop, with a convex side and the other tending to be flat.

From other diatom species worth mentioning, *Dactyliosolen tenuijunctus* (Fig. 4F, G) is a diatom lightly silicified and consequently difficult to see with inverted microscope; in most cases we identified it by its prominent and central nucleus, more evident than the frustule itself. *Eucampia antarctica* (Fig. 4A, B) was observed forming short straight chains. According to Scott and Thomas (2005), *Eucampia antarctica* var. *recta* is distinguished from *Eucampia antarctica* var. *antarctica* by its straight or slightly curved chains and its broader valve dimensions. Its distribution is restricted to Antarctica, probably an endemic species. Our specimens were identified as *Eucampia antarctica* var. *recta* denoting an Antarctic environment. *Cylindrotheca closterium* was observed only at near C-18a. We used the name *Cylindrotheca closterium* based on Medlin and Mann (2007), who proposed to keep the name *Cylindrotheca* instead of *Ceratoneis* for this taxon.

Small flagellated and coccoid cells were numerically the second most abundant group, after the diatoms. Kopczynska (1988) related the dominance of phytoflagellates over diatoms (mainly picoflagellates 1 to 3 μm in size) during spring, in waters of the Scotia Front, with areas of intensive water mixing and complex hydrography, arguing that the capacity of active movement would favor them. In her study she also included cryptophytes and prasinophytes in the phytoflagellate group. She reached similar conclusions with samples from Admiralty Bay, southern Drake Passage and Bransfield Strait. Later, Kopczynska (1992) also associated the dominance of unidentified flagellates, and sometimes of cryptophytes and prasinophytes, over diatoms with the occurrence of krill swarms. Cefarelli et al. (2010) reported unidentified small phytoflagellates ≤ 5 μm as a numerically dominant group in oceanic waters of the northern and eastern Weddell Sea, during summer. In spring, Bianchi et al. (1992) reported in closed pack ice zone, autotrophic nanoflagellates (single *Phaeocystis* cells, cryptophytes and *Pyramimonas* sp.) dominating numerically besides the small pennate diatoms. Similar to our results, these authors observed a general increment of flagellates with depth, including stations in oceanic waters.

Different taxa belonging to cryptophytes and prasinophytes have been found often characterizing the Antarctic nanoplankton (Kopczynska, 1992; Garibotti et al., 2003). However, in our samples they occurred in moderate concentrations. *Cryptomonas* species of different size (Fig. 4H) and *Pyramimonas* cf. *tychotreta* (Fig. 4I) are taxa difficult to identify to species level during cell counts since in general it requires culture studies and electron microscopy (Kopczynska, 1992). Dinoflagellates contribution to total biomass could be relatively high in comparison to their numerical abundance due to their large size.

Finally, it is worth noting that a filamentous blue-green alga was found and tentatively identified as *Anabaena* sp. (Fig. 4P, Q). It was found only in two stations at far C-18a and in a station at the control site. However, we could not distinguish heterocysts, characteristic of this taxon. As far as we know, a marine *Anabaena* species has not been cited for the Southern Ocean (Scott and Marchant, 2005). In Antarctica, *Anabaena* spp. have been found as subdominant components of cyanobacterial mats mainly in benthic community of lakes, streams, ponds and wetlands (Fernández-Valiente et al., 2001; Camacho and Fernández-Valiente, 2005). The genus is also found in the Baltic Sea, where planktonic *Anabaena* spp. are an important component of local cyanobacterial blooms (Sivonen et al. 1990; Suikkanen et al. 2010). In temperate waters of the western South Pacific Ocean, Arabian Sea and north of Australia, Carpenter and Janson (2001) detected a new *Anabaena* species (*A. gerdii*) in low concentrations, considering it one of the very few free-living heterocystous species present in the open sea. More material is necessary to determine identification and origin of this new material for Antarctic waters.

4.2. Effect of icebergs on phytoplankton distribution

Differences were observed among the four studied areas during the March-April cruise to the western Weddell Sea in 2009, both in species richness, as well as in abundance of the main taxonomic groups. The four areas of study were chosen along a gradient of "iceberg effect" with waters affected by numerous icebergs (Iceberg Alley) and where a large effect could be expected, near C-18a as waters affected by an isolated large iceberg, control site was the area where we expected less or no effect of icebergs and far C-18a was an area that the surface mapping and CTD transects away from the iceberg (Stephenson et al., 2011; Helly et al., 2011) indicated as having no influence from C-18a. Water masses analysis (Fig. 5) indicates that within the mixed layer, of most relevance to phytoplankton, water was coldest at Iceberg Alley and warmest at the control site, as might be expected from the influence of meltwater. However, the distribution of phytoplankton abundance and species richness were not as expected, lowest in the area of iceberg abundance (Iceberg Alley) and highest at the control site. The effect of one iceberg (near C-18a) was similar to the one at Iceberg Alley, with less intensity, and the area 18 km away from the iceberg (far C-18a) was more similar to the control area. Thus, there is a consistency between physics and phytoplankton response and results are organized along a temperature gradient, but the intensity of the signal is opposite to what was expected for algal biomass. Previous research on icebergs indicated a positive effect on phytoplankton biomass in the surrounding waters, where higher chlorophyll concentration was found ~1 km away from the iceberg (Smith et al., 2007) and where higher chlorophyll concentration was measured 6 days after an iceberg passage (Schwarz and Schodlok 2009). Both studies indicate an iceberg's positive influence during summer months, December 2005 (Smith et al., 2007) and November, December, January for 2000–2004 but not in October, February and March (Table 2 in Schwarz and Schodlok, 2009).

Meso-scale horizontal differences (< 20 km) in phytoplankton composition due C-18a presence were aligned with previous results. Diatoms are known to dominate productive areas in coastal waters (Cefarelli et al. 2010), the sea-ice edge (Garibotti et al., 2003) and sea ice (Garrison et al., 1987; Hegseth and von Quillfeldt, 2002). Their abundance near the iceberg supports the hypothesis that icebergs favor large phytoplankton (Smith et al., 2007). In addition, this study shows that small flagellates are significantly impoverished in waters close to C-18a, extending our understanding of how phytoplankton community composition responds to an iceberg.

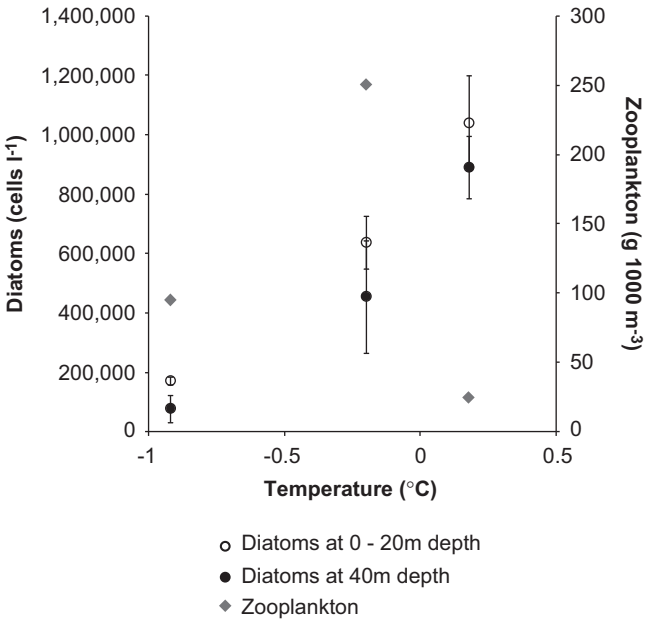

Fig. 8. Total average zooplankton abundance (g 1000 m^{-3}) and average diatoms (cells l^{-1}) along a temperature gradient defined, from low to high, by Iceberg Alley, near C-18a and Control (control site+far C-18a) (see also Table 3). 95% Confidence interval of zooplankton abundance is 47–100% of average biomass (not plotted for clarity; Kaufmann et al., 2011).

High flagellate abundance has been associated with lower salinity waters in polar regions, such as the Arctic Ocean (Li et al., 2009) and glacier meltwater in coastal waters of the western Antarctic Peninsula (Moline et al., 2004). This is in disagreement with our results of more flagellate concentration away from the iceberg. An alternative hypothesis, introduced by Kopczynska (1988) attributes lower stratification and turbulence to flagellate abundance, also opposite to our findings, as turbulence is expected to be higher at near C-18a. Isopycnals slope up away from the iceberg, while the surface density is nearly the same, so there is reduced stability (Stephenson et al., 2011), and lower small flagellated and coccoid cells close to the iceberg. Thus, flagellate distribution is either enhanced by bottom-up factors of higher salinity and reduced turbulence or is controlled by other factors, such as grazing. Unfortunately, we do not have microzooplankton grazing estimates nor heterotroph protists abundance, main grazers of small flagellates, to compare with our results.

The iceberg C-18a had a profound effect on the temperature and salinity of its surrounding waters. Stephenson et al. (2011) and Helly et al. (2011) identify three main physical processes in relation to the iceberg's dynamics, in particular melting and translation that can explain the gradients in temperature we observed. Iceberg melts in contact with warmer seawater. Basal melting, originating at the bottom of the iceberg, produces freshwater that rises towards the surface, mixing with surrounding water until reaching a depth of neutral density, usually at the depth of the winter water ~100 m (Stephenson et al., 2011). This type of turbulent mixing process is expected to affect phytoplankton below the mixed layer with an overall effect of decreasing temperature. Basal meltwater can also rise to the surface without mixing with surrounding waters (Donaldon, 1978; Neshyba, 1978), lowering surface salinity in the iceberg's vicinity. Low surface salinity and temperature near the iceberg was measured by surface mapping (Fig. 4, Helly et al., 2011). These conditions were observed at the iceberg's wake, extended for 19 km and were persistent for 10 days. A third proposed mechanism related to melting at the sides of the iceberg creating meltwater that mixed with surrounding waters at depth; through double diffusion this process resulted in increased salinity along isopycnals sloping up away from the iceberg (Stephenson et al., 2011). Meltwater and upwelling do not occur continuously but are observed as events or intrusions (Stephenson et al., 2011), providing a complex field of temperature and salinity. The observed low average temperature and associated low phytoplankton abundance at the mixed layer at the Iceberg Alley and near C-18a indicated that on average, the dominant process near the iceberg was one of meltwater cooling by upwelling and mixing, processes known to favor diatom growth (Rodriguez et al., 2001).

The net effect of the iceberg's presence at the depth of importance to phytoplankton composition and abundance, the mixed layer (within surface to 40 m) and the euphotic zone (within 80 to 105 m; Vernet et al., 2011), could be positive or negative depending on the strength of competing processes. We can expect lower phytoplankton abundance if the dilution effects counteract *in situ* growth. In contrast, we can expect higher biomass if increased mixing, or Fe enrichment originating from melting, favors growth (Coale et al., 2004; Boyd et al., 2007). Icebergs have been studied as a possible source of iron to the adjacent waters (de Baar et al., 1990; Smith et al., 2007) and surface meltwater from C-18a was enriched in Fe^{2+} (Lin et al., 2011). Thus, changes in phytoplankton composition close to the iceberg are in accordance to the main processes of mixing and melting associated with the iceberg, but cannot sustain higher phytoplankton density, with the exception of more diatom abundance at depth (~100 m). Further evidence of phytoplankton accumulating at this deep layer is the higher biomass of large cells (measured as chlorophyll $a > 10$ μm) observed around C-18a (Vernet et al., 2011). However, phytoplankton within the mixed layer was not more abundant close to the iceberg, reflecting either a growth rate lower than the dilution rate or another important loss term associated with the iceberg.

Low phytoplankton abundance close to the iceberg indicates that phytoplankton growth is lower than the *in situ* losses. This could explain the difference with published results on positive iceberg effects and could be related to a seasonal signal. If the enrichment in diatoms close to C-18a is interpreted as an indication of active growth, a high loss rate is controlling total abundance. The measured growth of 0.05 ± 0.03 d^{-1} (Vernet et al., 2011) or a division every ~20 days is not sufficient to counteract losses. Helly et al. (2011) calculated 2×10^{10} m^3 d is the volume of water swept by C-18a daily, entraining deep water from below 200 m and mixing with meltwater at a rate of 0.20–0.41% (Stephenson et al., 2011). These processes are expected to dilute phytoplankton biomass in the top 100 m and counteract daily growth, restricting biomass accumulation.

Another important loss could be due to zooplankton grazing. Zooplankton abundance was higher close to C-18a, in particular Antarctic krill and salps (Kaufmann et al., 2011), and lower in far C-18a and the control site. On average, zooplankton abundance was inversely related to diatom abundance (Fig. 8). Although any estimates of diatom consumption would be based only on zooplankton abundance, we can expect grazing to be higher next to the iceberg. Krill was concentrated in the upper 50 m of the water column (Kaufmann et al., 2011) and are known to prefer diatoms as food source (Kopczynska, 1992; Ross et al., 2000). Similarly, lower flagellate abundance near the iceberg could result from salp grazing (Dubischar and Bathmann, 1997). Zooplankton grazing as an important factor in controlling phytoplankton community is well documented for polar waters of the western Antarctic Peninsula (Haberman et al., 2003; Garibotti et al., 2003).

Based on results from this study we propose that the effect of icebergs on phytoplankton is a signal modulated by seasonal

processes, where net phytoplankton accumulation can be observed in periods of high growth but that becomes negligible during periods of lower growth (early spring) or at the end of the growth season where grazing by zooplankton dominates, is during this cruise (fall months).

5. Conclusions

A similar species composition was observed in the four studied areas within the Powell Basin, with significantly lower number of taxa at Iceberg Alley. *Fragilariopsis nana* was numerically the dominant taxon; however, its contribution to total phytoplankton biomass was relatively low due to its small size. Taxonomic analysis based on Scanning Electron Microscopy corroborated the similarity between *Fragilariopsis nana* and *F. cylindrus*, the former recently typified. We agree with Lundholm and Hasle (2008) that specimens previously identified as *F. cylindrus* could belong to either species. Therefore two different species could be dominant or co-dominant in Antarctica; further studies are needed to establish their differences in habitat.

The present study demonstrated also the effect of icebergs on phytoplankton, albeit different from what was expected from previous studies. Phytoplankton abundance, and to a lesser extent composition, correlated with meltwater from icebergs, as indicated by water temperature. Phytoplankton composition was positively affected by the iceberg and was function of depth: waters close to the iceberg were significantly impoverished in small flagellates at the mixed layer (surface-~40 m) and were enriched in diatoms at depth (~100 m). Phytoplankton abundance was negatively related to meltwater. Zooplankton grazing, originating from the large zooplankton biomass associated with icebergs, is hypothesized to control algal biomass close to the iceberg, although dilution by meltwater cannot be ruled out. These results indicate that icebergs can change the balance between phytoplankton growth and loss with respect to surrounding waters, and that this signal is modulated by seasons.

Acknowledgments

This study was supported in part by grants from the US National Science Foundation, awards ANT-0529815, ANT-0650034 to K. Smith and ANT-0636730 to M. Vernet. A.O. Cefarelli work was supported by a fellowship of the Universidad Nacional de La Plata, Argentina. We thank P. Sarmiento for her excellent technical assistance with SEM work in EM Service at the Museo de La Plata, Argentina. We extend our deep appreciation to the officers and crew on ARIB NB Palmer and the technical support from Raytheon Polar Services during sample collection. The authors acknowledge D. Chakos and K. Sines for assistance during sampling and W. Kozlowski for help with graphics. We thank Dr. R. Echenique for help on determining cyanobacterium species, to Dr. S. Bramardi for help with statistical analyses, to F. Gadomski for technical assistance, to D. Martinez for assistance during early stages of the manuscript preparation, to H. Isbert Perlender for the map, to Dr. R. Kaufmann for zooplankton data and to Dr. C. Gle for comments on the manuscript.

References

Arrigo, K.R., van Dijken, G.L., Ainley, D.G., Fahnestock, M.A., Markus, T., 2002. Ecological impact of a large Antarctic iceberg. Geophysical Research Letters 29, 1–4.

Ballantyne, J., 2002. A multidecadal study of the number of Antarctic icebergs using scatterometer data. BYU online report: http://www.scp.byu.edu/data/iceberg/IcebergReport.pdf.

Bianchi, F., Boldrin, A., Cioce, F., Dieckmann, G., Kuosa, H., Larsson, A.-M., Nöthig, E.-M., Sehlstedt, P.-I, Socal, G., Syvertsen, E.E., 1992. Phytoplankton distribution in relation to sea ice, hydrography and nutrients in the northwestern Weddell Sea in early spring 1988 during EPOS. Polar Biology 12, 225–235.

Boyd, P.W., Jickells, T., Law, C.S., Blain, S., Boyle, E.A., Buesseler, K.O., Coale, K.H., Cullen, J.J., de Baar, H.J.W., Follows, M., Harvey, M., Lancelot, C., Levasseur, M., Owens, N.P.J., Pollard, R., Rivkin, R.B., Sarmiento, J., Schoemann, V., Smetacek, V., Takeda, S., Tsuda, A., Turner, S., Watson, A.J., 2007. Mesoscale Iron Enrichment Experiments 1993–2005: Synthesis and Future Directions. Nature 315, 612–617.

Camacho, A., Fernández-Valiente, E., 2005. Un mundo dominado por los microorganismos. Ecología microbiana de los lagos antárticos. Ecosistemas 14 (2): http://www.revistaecosistemas.net/articulo.asp?Id=109.

Carpenter, E.J., Janson, S., 2001. *Anabaena gerdii* sp. nov., a new planktonic filamentous cyanobacterium from the South Pacific Ocean and Arabian Sea. Phycologia 40 (2), 105–110.

Cefarelli, A.O., Ferrario, M.E., Almandoz, G.O., Atencio, A.G., Akselman, R., Vernet, M., 2010. Diversity of the diatom genus *Fragilariopsis* in the Argentine Sea and Antarctic waters: morphology, distribution and abundance. Polar Biology 33, 1463–1484.

Coale, K.H., Johnson, K.S., Chavez, F.P., Buesseler, K.O., Barber, R.T., Brzezinski, M.A., Cochlan, W.P., Millero, F.J., Falkowski, P.G., Bauer, J.E., Wanninkhof, R.H., Kudela, R.M., Altabet, M.A., Hales, B.E., Takahashi, T., Landry, M.R., Bidigare, R.R., Wang, X.J., Chase, Z., Strutton, P.G., Friederich, G.E., Gorbunov, M.Y., Lance, V.P., Hilting, A.K., Hiscock, M.R., Demarest, M., Hiscock, W.T., Sullivan, K.F., Tanner, S.J., Gordon, R.M., Hunter, C.N., Elrod, V.A., Fitzwater, S.E., Jones, J.L., Tozzi, S., Koblizek, M., Roberts, A.E., Herndon, J., Brewster, J., Ladizinsky, N., Smith, G., Cooper, D., Timothy, D., Brown, S.L., Selph, K.E., Sheridan, C.C., Twining, B.S., Johnson, Z.I., 2004. Southern ocean iron enrichment experiment: Carbon cycling in high-and low-Si waters. Science 304, 408–414.

Crawford, R.M., Hinz, F., Honeywill, C., 1998. Three species of the diatom genus *Corethron* Castracane: Structure, distribution and taxonomy. Diatom Research 13, 1–28.

de Baar, H.J.W., 1995. Importance of iron for phytoplankton blooms and carbon-dioxide drawdown in the Southern-Ocean. Nature, 373–412.

de Baar, H.J.W., Buma, A.G.J., Nolting, R.F., Cadée, G.C., Jacques, G, Treguer, P.J., 1990. On iron limitation of the Southern Ocean: experimental observations in the Weddell and Scotia Seas. Marine Ecology Progress Series 65, 105–122.

Donaldson, P.B., 1978. Melting of Antarctic icebergs. Nature 275, 305–306.

Dubischar, C.D., Bathmann, U.V., 1997. Grazing impact of copepods and salps on phytoplankton in the Atlantic sector of the Southern Ocean. Deep-Sea Research 44, 415–433.

El-Sayed, S.Z., Fryxell, G.A., 1993. Phytoplankton. In: Friedmann, E.I. (Ed.), Antarctic Microbiology. Wiley-Liss, New York, pp. 65–122.

Estrada, M., Delgado, M., 1990. Summer phytoplankton distributions in the Weddell Sea. Polar Biology 10, 441–449.

Fernández-Valiente, E., Quesada, A., Howard-Williams, C., Hawes, I., 2001. N_2-fixation in cyanobacterial mats from ponds on the McMurdo Ice Shelf, Antarctica. Microbial Ecology 42, 338–349.

Ferrario, M.E., Sar, E.A., Sala, S.E., 1995. Metodología básica para el estudio del fitoplancton con especial referencia a las diatomeas. In: Alveal, K., Ferrario, M.E., Oliveira, E.C., Sar, E.A. (Eds.), Manual de Métodos Ficológicos. Universidad de Concepción, Concepción, pp. 1–23.

Ferrario, M.E., Almandoz, G., Licea, S., Garibotti, I., 2008. Species of *Coscinodiscus* (Bacillariophyta) from the Gulf of Mexico, Argentina and Antarctic waters: morphology and distribution. Nova Hedwigia, Beiheft 133, 187–216.

Fryxell, G.A., 1989. Marine phytoplankton at the Weddell Sea ice edge: Seasonal changes at the specific level. Polar Biology 10, 1–18.

Fryxell, G.A., Hasle, G.R., 1971. *Corethron criophilum* Castracane: Its distribution and structure. In: Llano, G.A., Wallen, I.E. (Eds.), Biology of the Antarctic Seas, vol. IV. American Geophysical Union, pp. 335–346.

Fryxell, G.A., Kendrick, G.A., 1988. Austral spring microalgae across the Weddell Sea ice edge; spatial relationships found along a northward transect during AMERIEZ 83. Deep-Sea Research 35, 1–20.

Garibotti, I.A., Vernet, M., Ferrario, M.E., Smith, R.C., Ross, R.M., Quetin, L.B., 2003. Phytoplankton spatial distribution in the western Antarctic Peninsula (Southern Ocean). Marine Ecology Progress Series 261, 21–39.

Garrison, D.L., Buck, K.R., Fryxell, G.A., 1987. Algal assemblages in Antarctic pack ice and in ice-edge plankton. Journal of Phycology 23, 564–572.

Gleitz, M., Kukert, H., Riebesell, U., Dieckmann, G.S., 1996. Carbon acquisition and growth of Antarctic sea ice diatoms in closed bottle incubations. Marine Ecology Progress Series 135, 169–177.

Gómez, F., 2007. The Consortium of the Protozoan *Solenicola setigera* and the Diatom *Leptocylindrus mediterraneus* in the Pacific Ocean. Acta Protozoologica 46, 15–24.

Haberman, K.L., Quetin, L.B., Ross, R.M., 2003. Diet of the Antarctic krill (*Euphausia superva* Dana): I. Comparisons of grazing on *Phaeocystis antarctica* (Karsten) and *Thalassiosira antarctica* (Comber). Journal of Experimental Marine Biology and Ecology 283, 79–95.

Hasle, G.R., Fryxell, G.A., 1970. Diatoms: cleaning and mounting for light and electron microscopy. Transactions of the American Microscopical Society 89, 468–474.

Hasle, G.R., Medlin, L.K., 1990. Family Bacillariaceae: the genus *Nitzschia* section *Fragilariopsis*. In: Medlin, L.K., Priddle, J. (Eds.), Polar Marine Diatoms. British Antarctic Survey, Natural Environment Research Council, Cambridge, pp. 181–196.

Hasle, G.R., Syvertsen, E.E., 1997. Marine diatoms. In: Tomas, C.R. (Ed.), Identifying marine phytoplankton. Academic Press, San Diego, pp. 5–385.
Hegseth, E.N., von Quillfeldt, C.H., 2002. Low phytoplankton biomass and ice algal blooms in the Weddell Sea during the ice-filled summer of 1997. Antarctic Science 14, 231–243.
Helly, J.J., Kaufmann, R.S., Stephenson, G., Vernet, M., 2011. Cooling, dilution and mixing of ocean water by free-drifting icebergs in the Weddell Sea. Deep-Sea Research II 58 (11-12), 1346–1363.
Hillebrand, H., Dürselen, CD., Kirschtel, D., Pollingher, U., Zohary, T., 1999. Biovolume calculation for pelagic and benthic microalgae. Jornal of Phycology 35, 403–424.
Holm-Hansen, O., Lorenzen, C., Holmes, R., Strickland, J., 1965. Fluorometric determination of chlorophyll. J. du Conseil 30, 3–15.
Jacobs, S.S., Gordon, A.L., Amos, A.F., 1979. Effect of glacial ice melting on the Antarctic surface water. Nature 277, 469–471.
Kang, S-H., Fryxell, G.A., 1991. Most abundant diatom species in water column assemblages from five Leg 119 drill sites in Prydz Bay, Antarctica: Distributional patterns. Proceedings of the Ocean Drilling Program, Scientific Results 119, 645–666.
Kang, S-H., Fryxell, G.A., 1992. *Fragilariopsis cylindrus* (Grunow) Krieger: The most abundant diatom in water column assemblages of Antarctic marginal ice-edge zones. Polar Biology 12, 609–627.
Kang, S-H., Fryxell, G.A., 1993. Phytoplankton in the Weddell Sea, Antarctica: composition, abundance and distribution in water-column assemblages of the marginal ice-edge zone during austral autumn. Marine Biology 116, 335–348.
Kaufmann, R.S., Robison, B.H., Sherlock, R.E., Reisenbichler, K.R., Osborn, K.J., 2011. Composition and structure of macrozooplankton and micronekton communities in the vicinity of free-drifting Antarctic icebergs. Deep-Sea Research II 58 (11-12), 1469–1484.
Knox, G.A., 2007. Biology of the Southern Ocean.. CRC Press, Boca Raton 621.
Kopczynska, E.E., 1988. Spatial structure of phytoplankton in the Scotia Front west Elephant Island (BIOMASS III, October-November 1986). Polish Polar Research 9, 231–242.
Kopczynska, E.E., 1992. Dominance of microflagellates over diatoms in the Antarctic areas of deep vertical mixing and krill concentrations. Journal of Plankton Research 14, 1031–1054.
Li, W.K.W., Mc Laughlin, F.A., Lovejoy, C., Carmack, E., 2009. Smallest algae thrive as the Arctic Ocean freshens. Science 326, 539.
Lin, H., Rauschenberg, S., Hexel, C.R., Shaw, T.J., Twining, B.S., 2011. Free-drifting icebergs as sources of iron to the Weddell Sea. Deep-Sea Research II 58 (11-12), 1392–1406.
Lizotte, M.P., 2001. The Contributions of Sea Ice Algae to Antarctic Marine Primary Production. American Zoologist 41, 57–73.
Long, D.G., Ballantyne, J., Bertoia, C., 2002. Is the number of icebergs around Antarctica increasing? EOS, Transactions, American Geophysical Union 42, 469–474.
Lundholm, N., Hasle, G.R., 2008. Are *Fragilariopsis cylindrus* and *Fragilariopsis nana* bipolar diatoms?—Morphological and molecular analyses of two sympatric species. Nova Hedwigia, Beiheft 133, 231–250.
Mc Minn, A., Scott, F.J., 2005. Dinoflagellates. In: Scott, F.J., Marchant, H.J. (Eds.), Antarctic marine protists. Australian Biological Resources Study, Canberra, pp. 202–250.
Medlin, L.K., Mann, D., 2007. 1783) Proposal to conserve the name *Cylindrotheca* against *Ceratoneis* (Bacillariophyceae). Taxon 56, 953–955.
Moline, M.A., Claustre, H., Frazer, T.K., Schofield, O., Vernet, M., 2004. Alteration of the food web along the Antarctic Peninsula in response to a regional warming trend. Global Change Biology 10, 1973–1980.
Montagnes, D.J.S., Berges, J.A., Harrison, P.J., Taylor, F.J.R., 1994. Estimating carbon, nitrogen, protein, and chlorophyll *a* from volume in marine phytoplankton. Limnology and Oceanography 39, 1044–1060.
Neshyba, S., 1977. Upwelling by icebergs. Nature 267, 507–508.
Neshyba, S., 1978. Melting icebergs. Nature 275 567–567.
Rines, J.E.B., Hargraves, P.E., 1988. The *Chaetoceros* Ehrenberg (Bacillariophyceae) flora of Narragansett Bay, Rhode Island, U.S.A. Bibliotheca Phycologica 79, 1–196.
Rodriguez, J., Tintore, J., Allen, J.T., Blanco, J.M., Gomis, D., Reul, A., Ruiz, J., Rodriguez, V., Echevarria, F., Jimenez-Gomez, F., 2001. Mesoscale vertical motion and the size structure of phytoplankton in the ocean. Nature 410, 360–362.
Ross, R.M., Quetin, L.B., Baker, K.S., Vernet, M., Smith, R.C., 2000. Growth limitation in young *Euphausia superba* under field conditions. Limnology and Oceanography 45, 31–43.
Round, F.E., Crawford, R.M., Mann, D.G., 1990. The diatoms, biology and morphology of the genera. Cambridge University Press, Cambridge, pp. 747.
Schodlok, M.P., Hellmer, H.H., Rohardt, G., Fahrbach, E., 2006. Weddell Sea iceberg drift: Five years of observations. Journal of Geophysical Research 111, 1–14.
Schwarz, J.N., Schodlok, M.P., 2009. Impact of drifting icebergs on surface phytoplankton biomass in the Southern Ocean: Ocean colour remote sensing and *in situ* iceberg tracking. Deep-Sea Research I 56, 1727–1741.
Scott, F.J., Marchant, H.J., 2005. Antarctic marine protists. Australian Biological Resources Study, Canberra, pp. 563.
Scott, F.J., Thomas, D.P., 2005. Diatoms. In: Scott, F.J., Marchant, H.J. (Eds.), Antarctic marine protists. Australian Biological Resources Study, Canberra, pp. 13–201.
Sivonen, K., Niemelä, S.I., Niemi, R.M., Lepistö, L., Luoma, T.H., Räsänen, L.A., 1990. Toxic cyanobacteria (blue-green algae) in Finnish fresh and coastal waters. Hydrobiologia 190, 267–275.
Smith, W.O., Nelson, D.M., 1985. Phytoplankton bloom produced by receding ice edge in the Ross Sea: spatial coherence with the density field. Science 227, 163–165.
Smith Jr., K.L., 2011. Free-drifting icebergs in the Southern Ocean; an overview. Deep-Sea Research II 58 (11-12), 1277–1284.
Smith Jr., K.L., Robison, B.H., Helly, J.J., Kaufmann, R.S., Ruhl, H.A., Shaw, T.J., Twining, B.S., Vernet, M., 2007. Free-drifting icebergs: hot spots of chemical and biological enrichment in the Weddell Sea. Science 317, 478–482.
Smith Jr., K.L., Sherman, A.D., Shaw, T.J., Murray, A., Vernet, M., Cefarelli, A.O., 2011. Carbon export associated with free-drifting icebergs in the Southern Ocean. Deep-Sea Research II 58 (11-12), 1485–1496.
Socal, G., Nöthig, E.M., Bianchi, F., Boldrin, A., Mathot, S., Rabitti., S., 1997. Phytoplankton and particulate matter at the Weddell/Scotia Confluence (47°W) in summer 1989, as a final step of a temporal succession (EPOS project). Polar Biology 18, 1–9.
Steidinger, K.A., Tangen, K., 1997. Dinoflagellates. In: Tomas, C.R. (Ed.), Identifying marine phytoplankton. Academic Press, San Diego, pp. 387–584.
Stephenson, G.R., Sprintall, J., Gille, S.T., Vernet, M., Helly, J., Kaufmann, R., 2011. Subsurface melting of a free-floating Antarctic iceberg. Deep-Sea Research II 58 (11-12), 1336–1345.
Suikkanen, S., Kaartokallio, H., Hällfors, S., Huttunen, M., Laamanen, M., 2010. Life cycle strategies of bloom-forming, filamentous cyanobacteria in the Baltic Sea. Deep-Sea Research II 57, 199–209.
Sunesen, I., Hernández-Becerril, D.U., Sar, E.A., 2008. Marine diatoms from Buenos Aires coastal waters (Argentina). V. Species of the genus *Chaetoceros*. Revista de Biología Marina y Oceanografía 43, 303–326.
Utermöhl, H., 1958. Zur Vervollkommnung der quantitativen Phytoplankton-Methodik. Mitteilungen der Internationale Vereinigung für Theoretische und Angewandte Limnologie 9, 1–38.
Vernet, M., Martinson, D., Iannuzzi, R., Stammerjohn, S., Kozlowski, W., Sines, K., Smith, R., Garibotti, I., 2008. Primary production within the sea-ice zone west of the Antarctic Peninsula: I—Sea ice, summer mixed layer, and irradiance. Deep-Sea Research II 55, 2068–2085.
Vernet, M., Sines, K., Chakos, D., Cefarelli, A.O., Ekern, L., 2011. Impacts on phytoplankton dynamics by free-drifting icebergs in the NW Weddell Sea. Deep-Sea Research II 58 (11-12), 1422–1435.
Villafañe, V.E., Helbling, E.W., Holm-Hansen, O., 1995. Spatial and temporal variability of phytoplankton biomass and taxonomic composition around Elephant Island, Antarctica, during the summers of 1990–1993. Marine Biology 123, 677–686.
Zar, J., 1996. Biostatistical analysis, 3rd edition Prentise Hall, New Jersey.